PROCEEDINGS, 49th Workshop on Geothermal Reservoir Engineering
Stanford University, Stanford, California, February 12-14, 2024
SGP-TR-227

Numerical Modeling of Stimulation and Circulation in Utah FORGE Wells

Sang H. Lee, Ahmad Ghassemi, Jonathan Ajo-Frankin*, and Matt Becker**

Reservoir Geomechanics and Seismicity Research Group, The University of Oklahoma, Norman, OK, USA

*Rice University, Houston, Texas, USA

**The California State University, Long Beach, California, USA

ahmad.ghassemi@ou.edu

Keywords: Geothermal, Reservoir Simulation, Discrete Fracture Network, Utah FORGE, EGS, Reservoir Stimulation, Seismicity.

ABSTRACT

In this paper we simulate fluid flow and energy transport associated with injector and producer doublet in the Utah FOEG EGS. The reservoir is a stimulated rock mass with a natural DFN and fractures created and/or activated during the 3-stages of hydraulic stimulation and fracturing of the injection Well16A(78)-32. The paper focuses on the fluid circulation tests between wells 16A and 16B carried out in July 2023 in the Utah FORGE. The main objective of this study is to estimate the reservoir permeability that would yield the pressure response recorded in 16B and the flow rates observed in 16A. The simulations consider the field data from the Circulation Test 1 (July 4th and 5th, 2023) and the Circulation Test 2 (July 18th – 20th, 2023). The reservoir model is constructed using the Utah FORGE native state data and subsequent stimulation outcomes obtained from observed micro-seismicity and injection pressure data from the stimulation stages of April 2022. The simulation domain is discretized using irregular grid-blocks in a finite-difference scheme. Numerical calibration of the permeability using the pressure data and injection rate partitioning into the 3 stimulated stages show good agreement with the Utah FORGE circulation test data based on spinner data for the second circulation test (test 2, July 19th, 2023). The study helps characterization of the stimulation outcome and the rock mass transport properties in the Utah FORGE EGS and provides a basis for future modeling of planned stimulation and circulation tests.

1. INTRODUCTION

We previously demonstrated numerical finite-difference modeling of water circulation in the planned Utah FORGE doublet consisting of a hydraulic fractured injection well and a production well, accounting for the fluid flow and thermal energy transport. For the model verifications, we presented cold water injection into the fractured hot rock with a coupled fracture/reservoir model using the equivalent permeability approach (Lee and Ghassemi, 2023) to simulate lab-scale EGS experiments (Hu and Ghassemi, 2016, 2017, 2018, 2020) and Utah FORGE reservoir permeability resulting from stimulation (Lee and Ghassemi, 2022).

In this work, we present numerical modeling of fluid circulation tests between the Well16A(78)-32 and the Well16B(78)-32 by focusing on the injection-induced permeability increase and pressure change around the fluid circulation zones. The influence of pressure change and effective stress on permeability has been extensively studied and they proposed models for the relationship that the induced-pressure increase causes the permeability increases (Jones, 1988; Nethenson, 1999; Rutquivist et al., 2002). The permeability increases in response to induced-pressure increases are considered in this work. The simulation model is calibrated based on a total of 4 FORGE circulation tests (2 circulation tests were performed on July 4th and 5th, 2023, and the other 2 circulation tests were carried out on July 18th - 20th, 2023). The first 2 circulation tests were in the openhole section of the Well16B(78)-32 (Figure 1(a)), and the next 2 circulation tests were performed with the cased completion zone to 10,208 ft, MD, and 739 ft openhole below 10,208 ft, MD as shown in Figure 1(b).

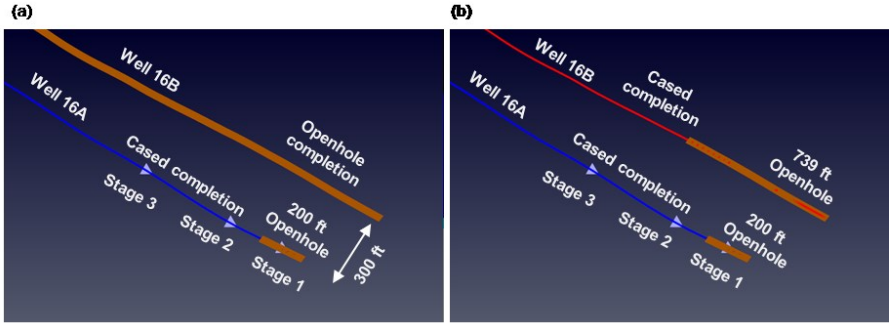

Figure 1: The description for circulation test in Utah FORGE injector (Well16A(78)-32) and production well (Well16B(78)-32. (a) Circulation test 1 is carried out on July 4th and 5th, 2023 with Well16B(78)-32 openhole condition. (b) Circulation test 2 is carried out on July 18th – 20th, 2023 with cased hole condition up to 10, 208 ft, MD, and 739 ft openhole below 10,208 ft, MD.

2. NUMERICAL MODELING

As described in the previous section, the numerical modeling focuses on the 4 circulation tests in Utah FORGE. To improve the simulation of fluid flow and energy transport in the model we rely on grid-blocks oriented in the inclined well coordinates. This was done by applying coordinate transformation to the permeabilities in the global coordinates using the Equation (1) – (3) based on the well azimuth (65°) and inclination (N110°E). The coordinate transformation begins with rotation for well inclination with respect to the y-axis using Equation (2), then rotate to the azimuth direction with respect to the z-axis using the Equation (3) (Hearn and Baker, 1996).

$$R_x(\theta) = \begin{pmatrix} 1 & 0 & 0 \\ 0 & \cos\theta & -\sin\theta \\ 0 & \sin\theta & \cos\theta \end{pmatrix} \quad (1)$$

$$R_y(\theta) = \begin{pmatrix} \cos\theta & 0 & \sin\theta \\ 0 & 1 & 0 \\ -\sin\theta & 0 & \cos\theta \end{pmatrix} \quad (2)$$

$$R_z(\theta) = \begin{pmatrix} \cos\theta & -\sin\theta & 0 \\ \sin\theta & \cos\theta & 0 \\ 0 & 0 & 1 \end{pmatrix} \quad (3)$$

To assess the fractional flow distributions in each stage during the circulation tests, we introduced the irregular grid-block model to simulate the fluid flow and energy transport within the wellbore (cased or openhole completion), as well as the pressure and temperature change around the circulation zone between the injector and the production well. The minimum grid-block length used is 0.22 m in y- and z-directions to model the 8.75-inch hole size, and the maximum grid-block length within the reservoir is limited to 20 m for the modeling. The constant grid-block size of 10 m is used for x-direction because no refinement is needed in the direction parallel to the wellbore. The total number of grid-blocks are 65, 61 and 81, respectively and the simulation domain size is 650m×608.8m×638.8m. The model domain and the cross-sectional view of grid-blocks is described in Figure 2. The schematic diagram of well locations and its grid-block configurations for coordinate transformations are illustrated in Figure 3.

Note that the initial permeability distribution is obtained from the discrete fracture network (DFN) equivalent permeability and the stimulated volume is constrained based on the microseismicity data around Stage 1, 2, 3 stimulations. For the wellbore grid-blocks, the model uses an ultra-high permeability (10^6 Darcy), and an ultra-low permeability (10^{-9} md) to simulate the cased hole walls. It is observed that the stimulated volumes are overestimated if we include all seismic events, so we filtered out several outliers during the calibration work as described in Figure 4. The input parameters used for simulations are listed in Table 1. Aside from its permeability, the reservoir state is assumed to be the native state i.e., temperature and pore pressure disturbance have dissipated.

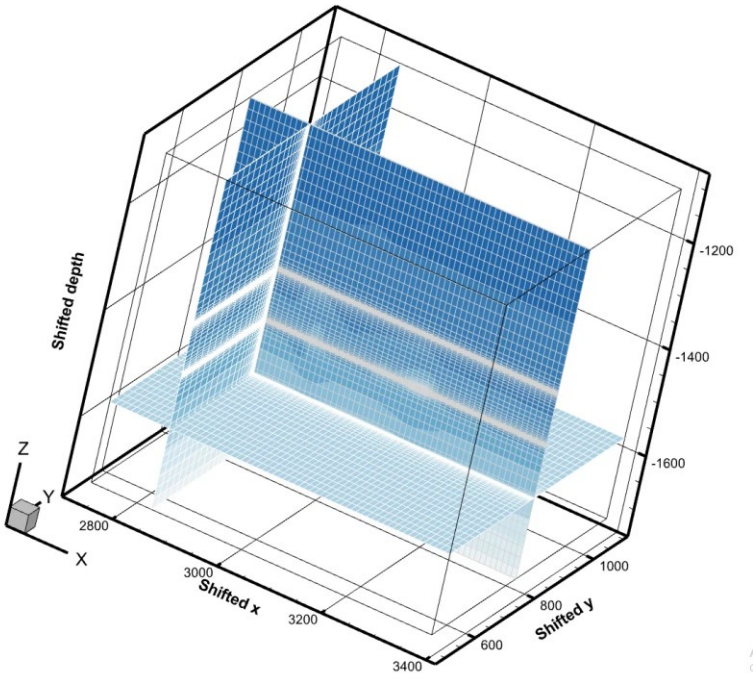

Figure 2: Discretized gid model in SI units. The grid block sizes are varied from 0.22 m to 20 m to improve the numerical model efficiency and quality for inclined wells.

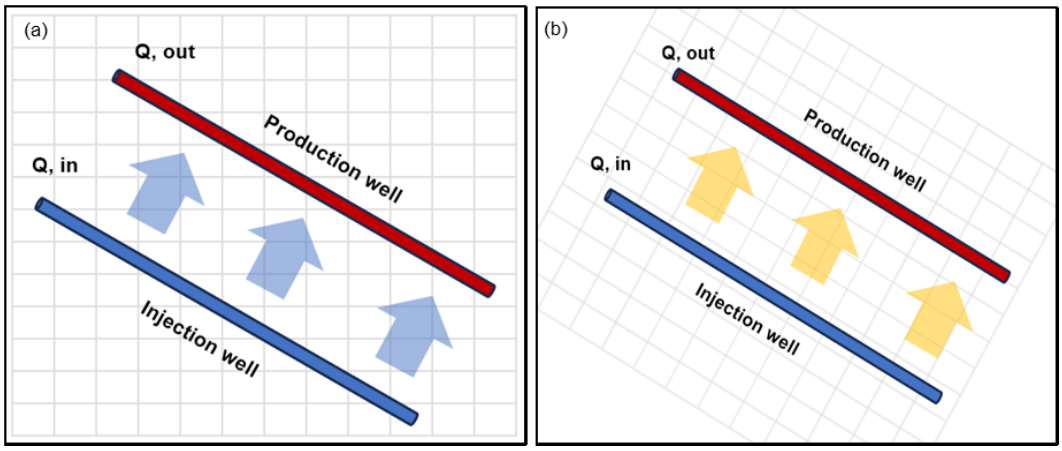

Figure 3: Schematic diagram of well flow between the North-East Cartesian coordinates and the coordinates transformation based on the well inclination and the azimuth. (a) North-East Cartesian coordinates, (b) coordinates transformation based on the inclination and the azimuth.

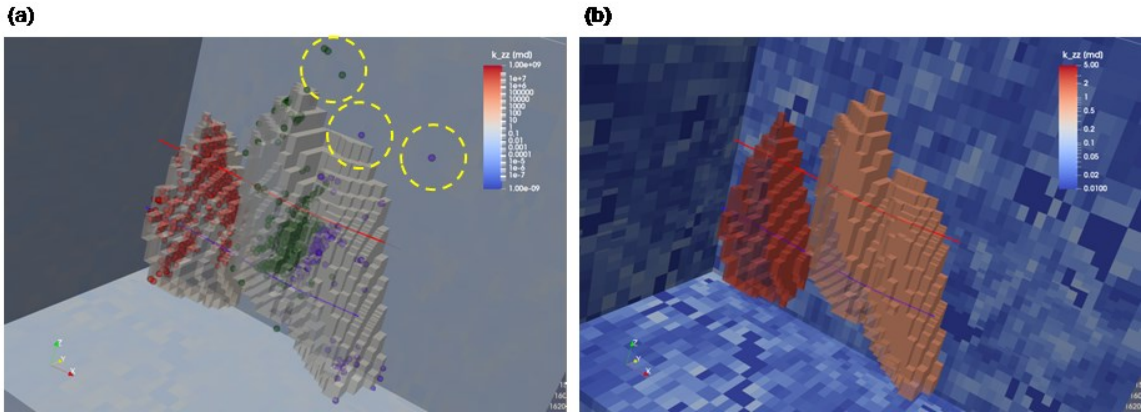

Figure 4: (a) Microseismic events data and stimulated volume. The outliers are marked as yellow circles and filtered out during the calibration work to improve the results. (b) DFN permeability distribution and high permeability zones around Stage 1, 2, 3.

Table 1: Input parameters for Utah FORGE stimulation modeling

Parameter	**Value**
Porosity, $\emptyset$	1 %
Thermal conductivity,	4.0 W/m-K
Matrix permeability, K	Discrete Fracture Network upscaled permeability distribution
Heat Capacity,	1200 J/Kg-K
Density of rock,	2.7 g/cm^3
Residual saturation of water,	0.30
Residual saturation of steam,	0.05

2.1 Numerical Modeling for Circulation Test 1

Drilling of the Well16A(78)-32 was completed in 2021, and it was stimulated in April 2022. Then, the production Well 16B(78)-32 was drilled to 10,947 ft, MD (8357 ft, TVDKB) in April 2023. The 11.75 inch casing shoe is at 4,837 ft, MD (total 6,110 ft openhole condition below 4,847 ft, MD) in Circulation Test 1. The injection Well16A(78)-32 is cased with a 200 ft openhole condition below 10,787 ft, MD. Two circulation tests have been performed on July 4th and 5th, 2023.

The wellhead pressure and injection rates used for calibration of the model (the injection rate in Well16A(78)-32 and the pressure in the production Well16B(78)-32) are presented in Figure 5 and the permeability changes with the injection rate are plotted in Figure 6. We calibrate the permeability based on the pressure response to the prescribed injection rate. It is observed that pressure and permeability increase as the injection rate increases. The pressure initially increases and then decreases slowly after 500 min because of the fracture reopening, and this is interpreted as permeability increases as plotted in Figure 6(a) and (b). Note that the Well16B(78)-32 pressure increases as the fluid is injected into the Well 16A(78)-32. Consistent with the field data, a fixed pressure condition is applied after 500 min of circulation. An isotropic permeability is used in the SRV of Stage 1 and Stage 2 based on the microseismic events cloud, ranging from 0.40 to 0.94 md. For Stage 3, anisotropic permeability is used based on the Stage 3 seismic events cloud and the fact that well-defined hydraulic fracture(s) are evident in the seismic data. Specifically, the anisotropy ratio is 1:30:15(k_{xx}, k_{yy}, k_{zz}). Note that because of the coordinate system used in this work, the anisotropic permeability directions are based on the well inclination and the azimuth, not the North-East direction. Comparing the calibrated permeability from the stimulation modeling of the 3 fracturing stages with those from the circulation test, we find the latter to be relatively lower. The main reason for the lower permeability is the lower injection rates for the circulation test compared to the stimulation activities in April 2022. Also, the finer grid blocks used (0.22 m vs 10 m regular grid-block for stimulation modeling) contribute to the differences. Pressure variations during Circulation Test 1 are presented in Figure 7. The pressure changes are more localized around the injection zones in the early stages and dissipate slowly as the injection rate decreases.

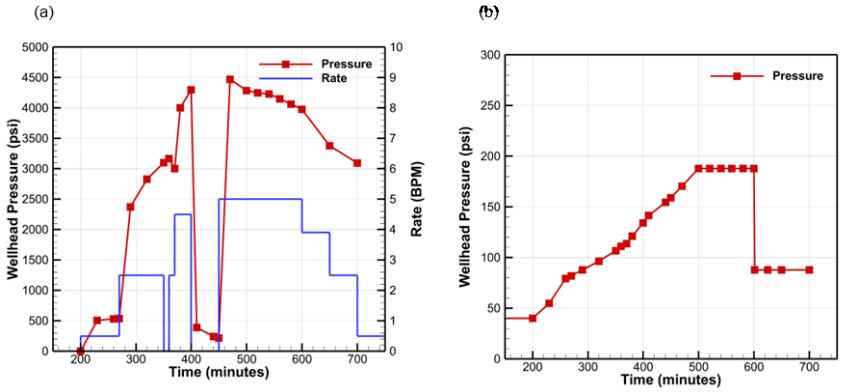

Figure 5: Pressure results for the first Circulation Test 1 (red line – pressure, blue line – injection rate): (a) model calibration for Well16A(78)-32 based on the injection rate and pressure response, (b) calibration for Well16B(78)-32. Pressure boundary conditions are applied after 500 min as indicated by field data (hold 16B pressure limit).

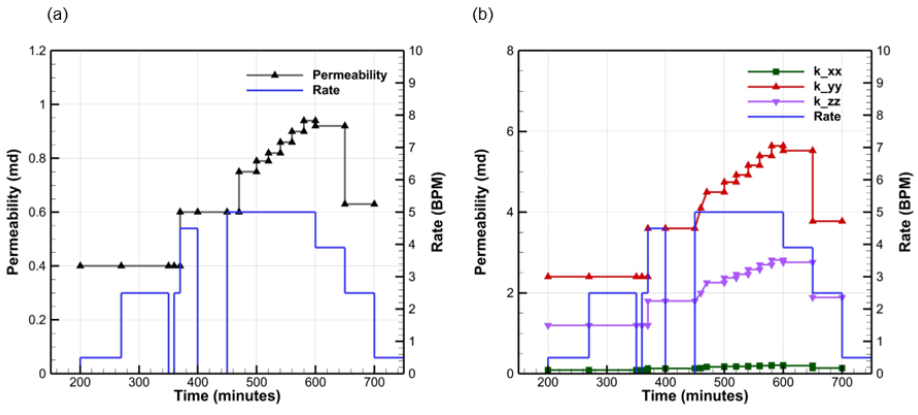

Figure 6: Permeability results for the first Circulation Test 1: (a) Permeability model around Stage1 and 2. The isotropic permeability model has been implemented to match the isotropic microseismic events clouds. The permeability ranges from 0.40 md to 0.94 md. (b) Permeability model around Stage 3. The anisotropic permeability model has been implemented to match the anisotropic microseismic events cloud. The calibrated anisotropic permeability for k_{xx} = 0.09 – 0.21 md, k_{yy} = 2.40 – 5.64 md, k_{zz} = 1.20 – 2.82 md.

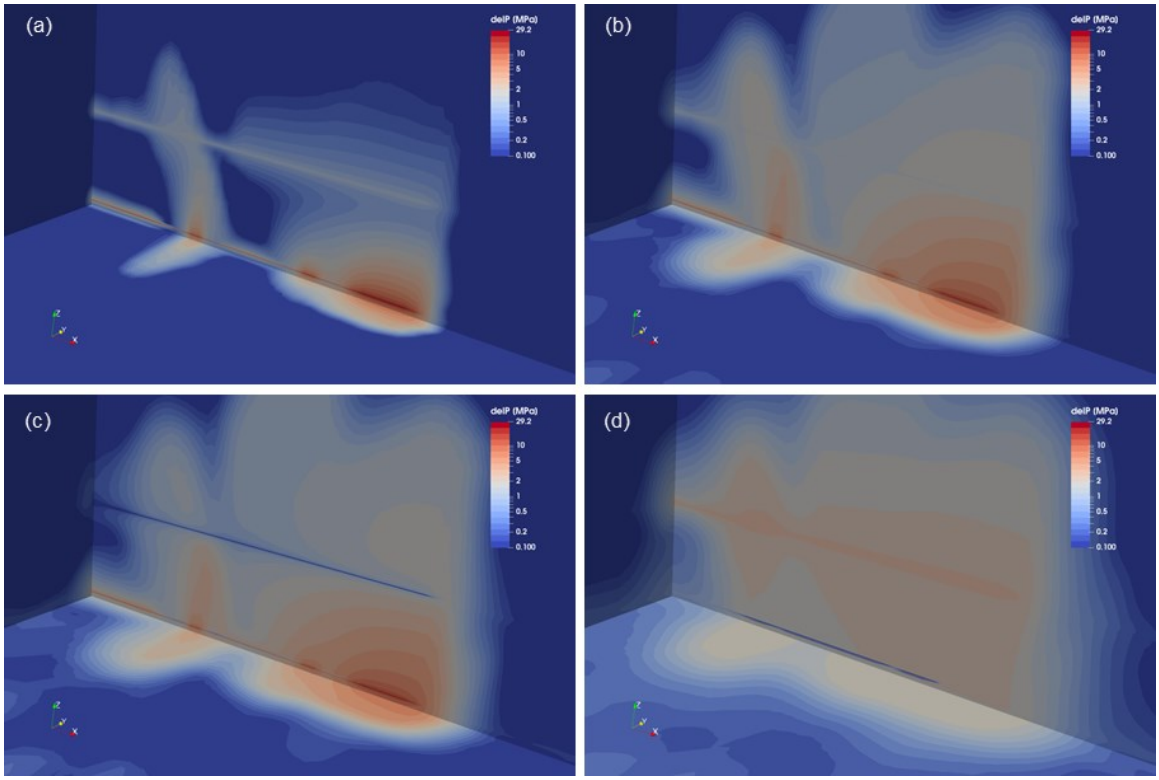

Figure 7: The change of pressure distributions for the Circulation Test 1 are plotted. (a) t = 270 min, (b) t = 350 min, (c) t = 470 min, (d) t = 700 min.

For Circulation Test 1, an injection rate of 5 BPM is used for 400 min while the production Well16B(78)-32 pressure was held at 200 psi for 300 min, and then the pressure was controlled stepwise up to 500 psi from 400 min to 950 min. The numerical model follows field test conditions, and the numerical pressure predictions for the injector with 5 BPM injection rate is presented in Figure 8(a). The pressure boundary conditions for the production well and the corresponding flow rates at different time-steps are also plotted in Figure 8(b). It is observed that the pressure increases rapidly for 50 min and then decreases slowly until circulation test is finished. The pressure behavior for the constant rate indicates that the fracture is reactivated during the circulation test. The calibrated permeability shows gradual increase in all 3 stimulation stages as plotted in Figure 9. The permeability ranges from 0.55 md to 0.98 md for Stage 1 and 2, and k_{xx} =0.11 – 0.22 md, k_{yy} =3.00 – 5.88 md, k_{zz} =1.50 – 2.94 md for Stage 3. 3D plots for pressure changes in the reservoir at different time-steps are presented in Figure 10.

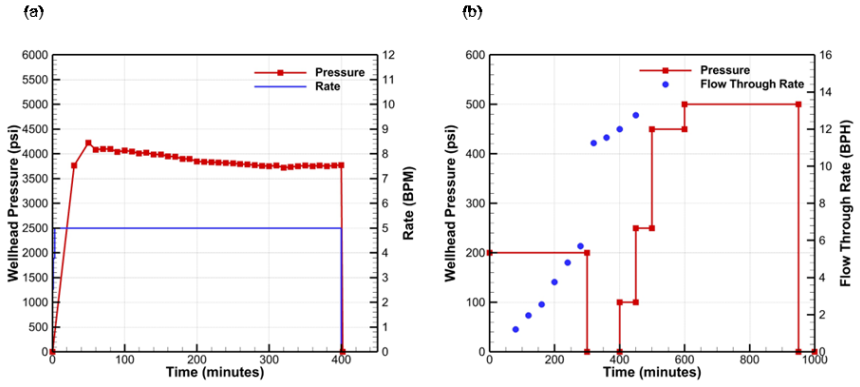

Figure 8: Plots of pressure modeling results for the second Circulation Test 1: (a) model calibration for Well16A(78)-32 based on the injection rate and pressure response, (b) calibration for Well16B(78)-32. Pressure boundary conditions are applied after 500 min as indicated by field data (hold 16B pressure limit). The flow through rate for Well16B(78)-32 is also plotted with blue dots.

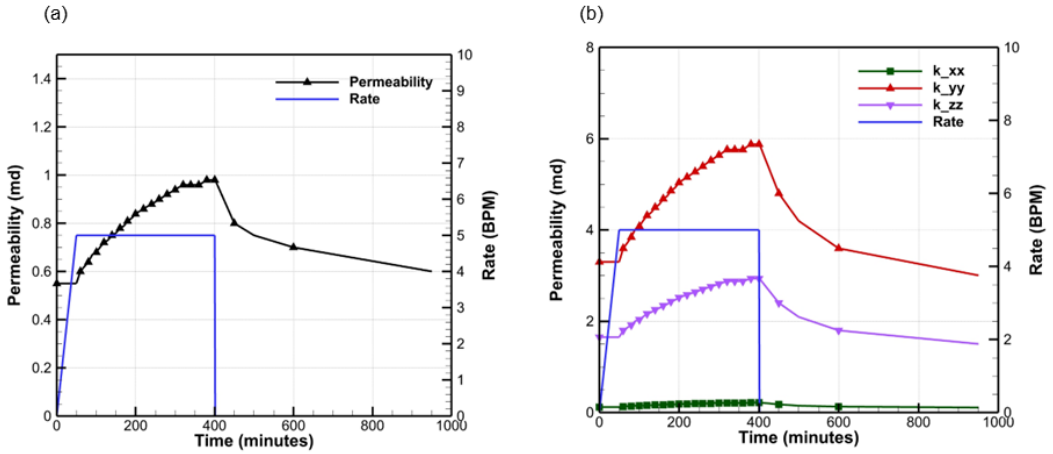

Figure 9: Plots of the permeability results for the second Circulation Test 1: (a) Permeability model around Stage 1 and 2. The isotropic permeability model has been implemented to match the isotropic microseismic events clouds. The permeability ranges from 0.55 md to 0.98 md. (b) Permeability model around Stage 3. The anisotropic permeability model has been implemented to match the anisotropic microseismic events cloud. The calibrated anisotropic permeability for k_{xx} = 0.11 – 0.22 md, k_{yy} = 3.00 – 5.88 md, k_{zz} = 1.50 – 2.94 md.

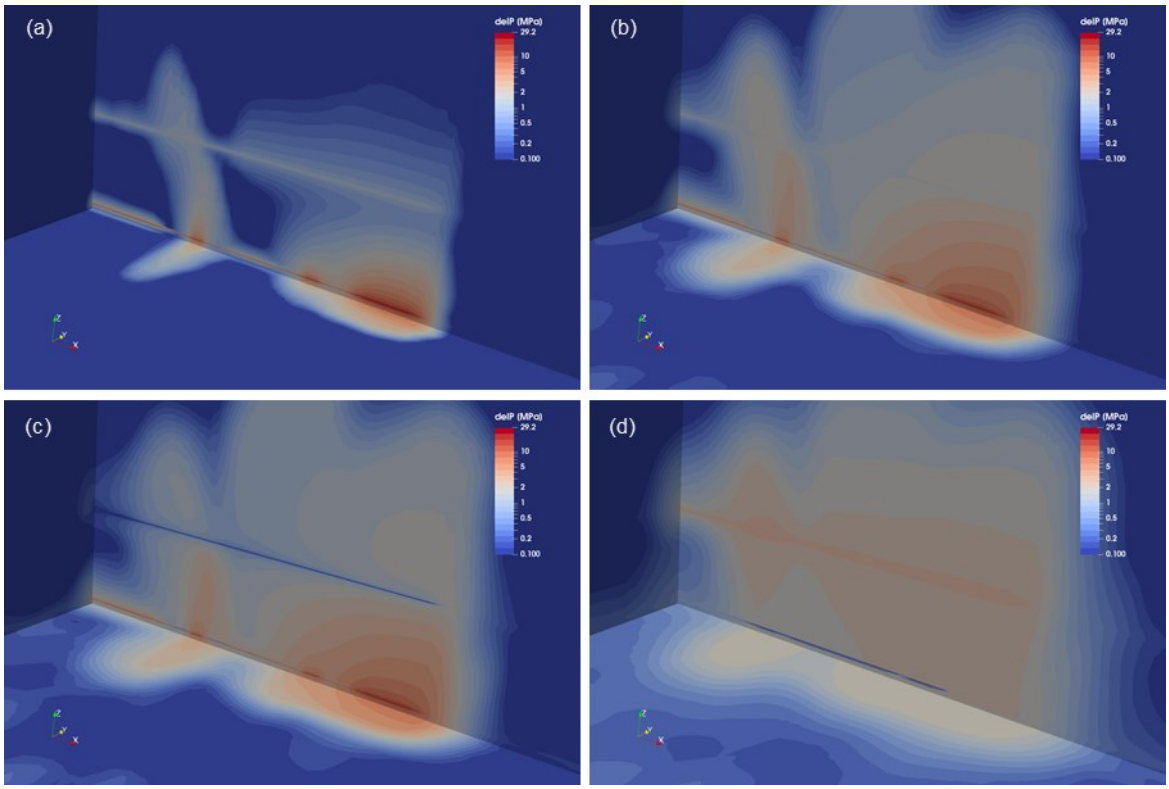

Figure 10: The change of pressure distributions for the second Circulation Test 1 are plotted. (a) t = 50 min, (b) t = 300 min, (c) t = 400 min, (d) t = 950 min.

2.2 Numerical Modeling for Circulation Test 2

After two circulation tests in July 4th and 5th, 2023 (Circulation Test 1), the Well16B(78)-32 was cased to 10,208 ft, MD as described in Figure 11(b), and two Circulation Test 2 is performed between July 18th – 20th, 2023. The injection rate increased up to 7.5 BPM compared to the 5.0 BPM for the Circulation Test 1. In the simulations, we use the ultra-low permeability value of 10^{-9} md around the production

wellbore while allowing for openhole conditions below 10,208 ft, MD. Pressure modeling for the first Circulation Test 2 is plotted in Figure 11(a) and the permeability model calibrations for Stage 1, 2, 3 are plotted in Figure 11(b). The pressure response with respect to the injection rate is similar to the Circulation Test 1. It is observed that the pressure increases rapidly at the onset of injection and then decreases slowly as illustrated in Figure 11(a). The permeability ranges from 0.30 md to 1.40 md for Stage 1 and 2, (0.07 – 0.31 md, 1.80 – 8.40 md, 0.90 – 4.20 md) for Stage 3 corresponding to k_{xx}, k_{yy}, k_{zz}, respectively. It noted that the Circulation Test 2 used a higher injection rate compared to the Circulation Test 1 (7.5 BPM vs 5.0 BPM). The calibrated maximum permeability is also increased by 40 – 42% compared to the second Circulation Test 1. The numerical model results for pressure changes are presented in Figure 13.

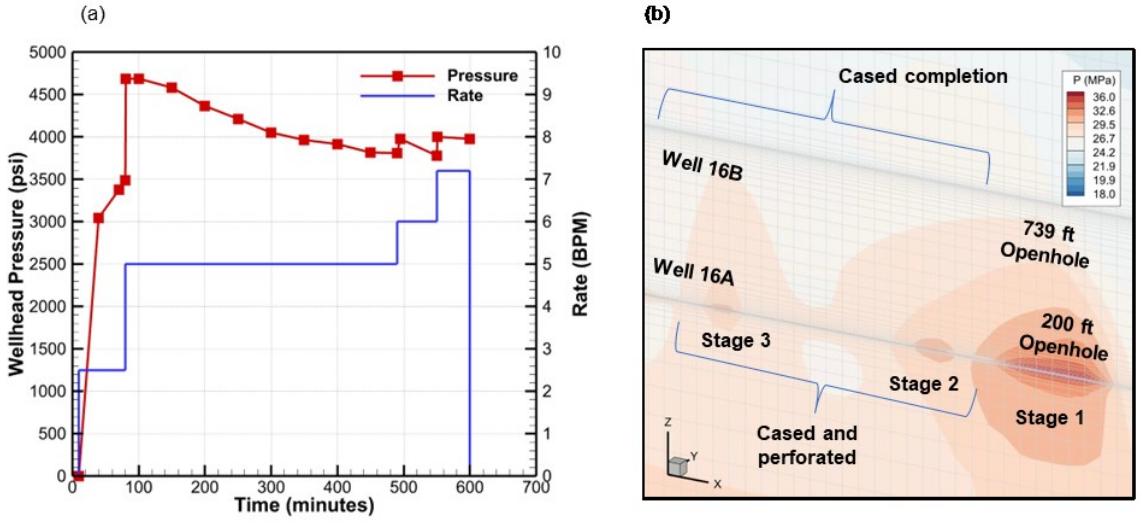

Figure 11: Pressure modeling results for the first Circulation Test 2 in (a), and the cross-sectional view around circulation zones including the irregular grid-blocks is presented in (b).

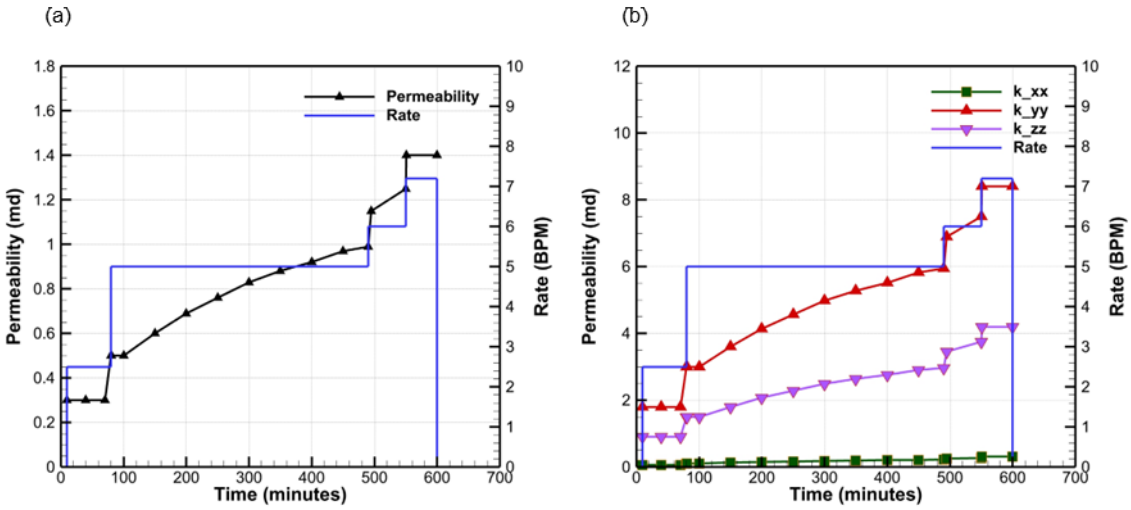

Figure 12: Permeability modeling results for the first Circulation Test 2: (a) Permeability model around Stage1 and 2. The isotropic permeability model has been implemented to match the isotropic microseismic events clouds. The permeability ranges from 0.30 md to 1.40 md. (b) Permeability model around Stage 3. The anisotropic permeability model has been implemented to match the anisotropic microseismic events cloud. The calibrated anisotropic permeability for k_{xx} = 0.07 – 0.31 md, k_{yy} = 1.80 – 8.40 md, k_{zz} = 0.90 – 4.20 md.

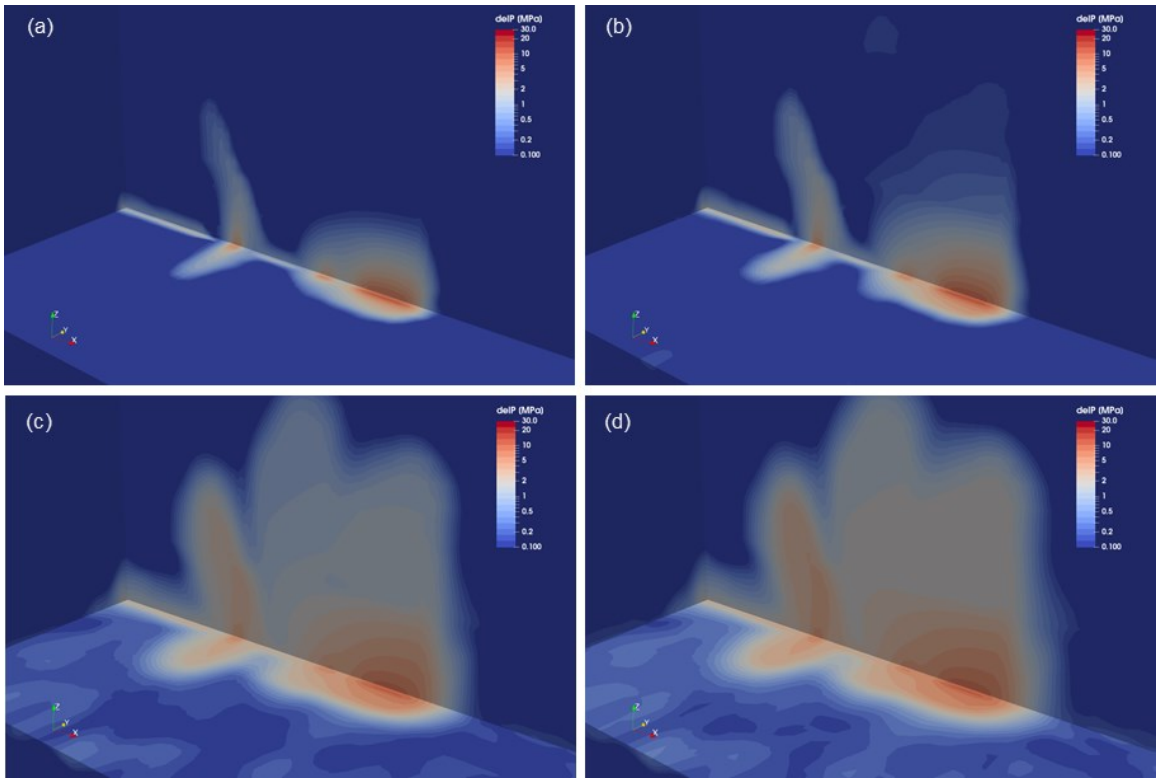

Figure 13: The change of pressure distributions for the first Circulation Test 2: (a) t = 70 min, (b) t = 120 min, (c) t = 420 min, (d) t = 590 min.

For the second test of Circulation Test 2, the injection rate was increased from 2.5 BPM to 7.5 BPM as plotted in Figure 14(a). The pressure response with respect to the injection rate is similar to other Circulation Tests, and the calibrated permeability model also has similar values. The permeability ranges from 0.28 md to 1.37 md for Stage 1 and 2, and (0.06 – 0.30 md), (1.68 – 8.22 md), (0.84 – 4.11) md for Stage 3 k_{xx}, k_{yy}, k_{zz}, respectively. It is noted that the spinner data measured on July 19th, 2023 indicate a flow partition of 44 – 50 % into Stage 1, and 30 – 40% into Stage 3. The data show different fractional flow rates for different circulation rates. For Stage 1, the fractional flow rate decreases as the circulation rate increases, but on the other hand, Stage 3 shows the opposite trend. The fractional flow rate is increased as the circulation rate is increased for Stage 3. The complexity of rock permeability including the interaction of natural fractures and hydraulic fractures between the injector and the production enhances the difficulty of interpretations. However, the observed phenomenon could be attributed to more favorable fracture orientation in Stage 3 that open in response to increased injection rate compared to Stage 1 which may be dominated with pre-existing natural fracture permeability.

The numerical results provide the fractional flow for each stage around the injector Well16A(78)-32, as shown in Figure 14(b). It is observed that the numerical results differ from field data by 5-10%, however the overall trend of the fractional flow rate variaions with respect to the injection rate are in very good agreement with field observations.

The 3D numerical results at different time-steps are illustrated in Figure 16. Similar to other circulation test results, the pressure diffusion pattern indicates insufficient connectivity between the injector and the producer. Therefore, stimulation of the injector and the producer or both would be necessary to improve connectivity.

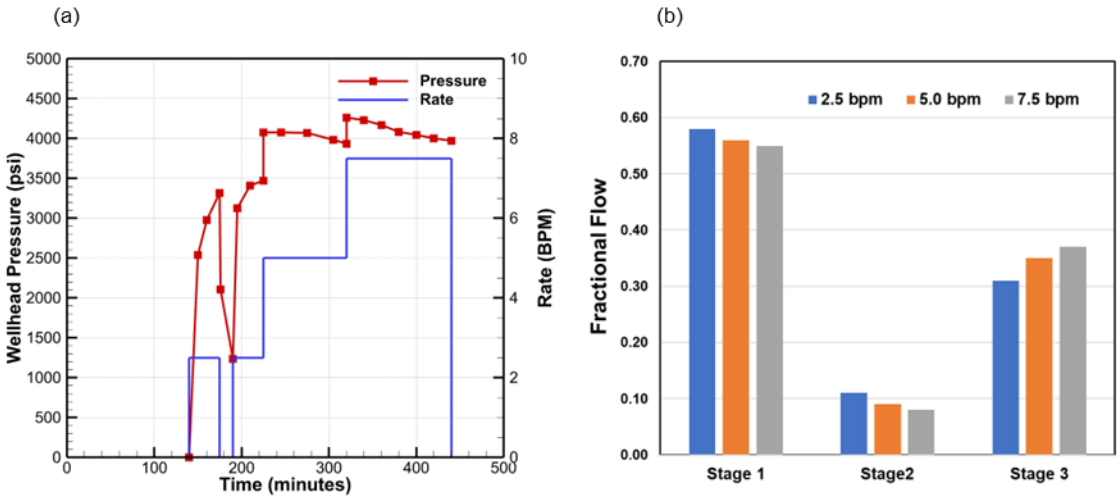

Figure 14: Pressure modeling results for the second Circulation Test 2 in (a), and the fractional flow rate modeling for different injection rates is presented in (b).

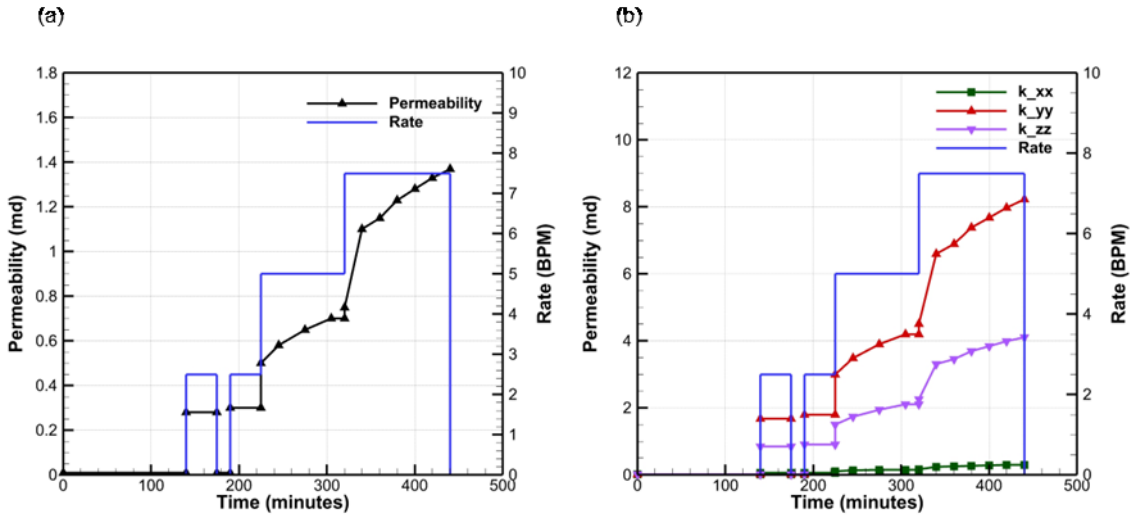

Figure 15: Permeability modeling results for the second Circulation Test 2: (a) Permeability model around Stage1 and 2. The isotropic permeability model has been implemented to match the isotropic microseismic events clouds. The permeability ranges from 0.28 md to 1.37 md. (b) Permeability model around Stage 3. The anisotropic permeability model has been implemented to match the anisotropic microseismic events cloud. The calibrated anisotropic permeability for k_{xx} = 0.06 – 0.30 md, k_{yy} = 1.68 – 8.22 md, k_{zz} = 0.84 – 4.11 md.

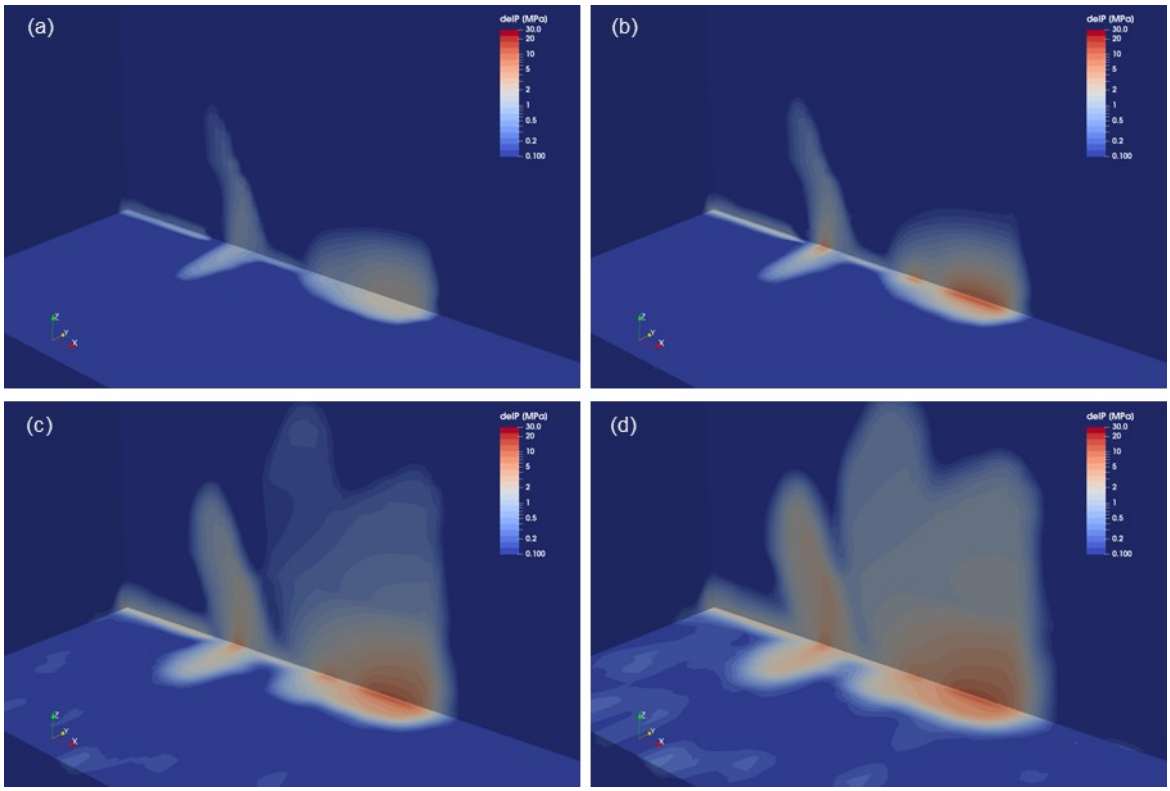

Figure 16: The change of pressure distributions for the second Circulation Test 2: (a) t = 190 min, (b) t = 225 min, (c) t = 320 min, (d) t = 440 min.

3. CONCLUSIONS

Fluid circulation in the Utah FORGE doublet has been studied using a coupled fracture/reservoir model for EGS with the capability to simulate two-phase water pressure, temperature and enthalpy change. Simulations consider DFN permeability and the stimulated volume based on the microseismic events by the Well16A(78)-32. The numerical modeling was carried out with the coordinates transformation to allow the consideration of inclined injector and producer wells, which improved the numerical result for fluid flow and energy transport between the grid-blocks during circulations. The irregular grid-blocks schemes were also implemented to increase the numerical model quality for pressure change around the wellbore. The simulation of the July 2023 circulation tests was used to estimate the reservoir permeability and transport capacity of the stimulated zones within 16A and the quality of the hydraulic connection with 16B. The results are in very good agreement with field data and underscore the need for additional stimulation to improve the connection between the doublet. Future work will consider optimization of the numerical modeling parameters based on distributed acoustic sensing (DAS) field data, to demonstrate the characterization of FORGE reservoir.

ACKNOWLEDGEMENTS

This project was supported by the Utah FORGE project sponsored by the U.S. Department of Energy, through the project "Fiber-Optic Geophysical Monitoring of Reservoir Evolution at the FORGE Milford Site."

REFERENCES

Hearn, D. and Baker, M. "Computer Graphic (2nd Edition)" Prentice Hall (1996)

Hu, L. and Ghassemi, A. "Laboratory Scale Investigation of Enhanced Geothermal Reservoir Stimulation." 50th U.S. Rock Mechanics/Geomechanics Symposium, Houston, TX (2016)

Hu, L. and Ghassemi, A. "Experimental Investigation of Hydraulically Induced Fracture Properties in Enhanced Geothermal Reservoir Stimulation." 42nd Workshop on Geothermal Reservoir Engineering Stanford University, Stanford, CA (2017)

Hu, L. and Ghassemi, A. "Heat and Fluid Flow Characterization of Hydraulically Induced Fracture in Lab-Scale." 52nd U.S. Rock Mechanics/Geomechanics Symposium, Seattle, WA (2018)

Hu, L., Ghassemi, A., Pritchett, J., Garg, S. "Characterization of laboratory-scale hydraulic fracturing for EGS." SPE Formation and Evaluation, (1988)

Hu, L. and Ghassemi, A. "Two-Point Determinations of Permeability and PV vs. Net Confining Stress" International Journal of Rock Mechanics and Mining Sciences, 126 (2020), 104205

Jones, S. C., "Heat production from lab-scale enhanced geothermal systems in granite and gabbro." International Journal of Rock Mechanics and Mining Sciences, 126 (2020), 104205

Lee, S. and Ghassemi, A. "Numerical Simulation of Fluid Circulation in Hydraulically Fractured Utah FORGE Well" 47th Workshop on Geothermal Reservoir Engineering Stanford University, Stanford, CA (2022)

Lee, S. H., Ratnayake, R. Ghassemi, A., "Numerical Analysis of Flow in Stimulated Utah FORGE Reservoir" GRC Transactions, 46 (2022).

Lee, S. and Ghassemi, A. "Modeling and Analysis of Stimulation and Fluid Flow in the Utah FORGE Reservoir" 48th Workshop on Geothermal Reservoir Engineering Stanford University, Stanford, CA (2023)

Lee, S. H. and Ghassemi, A., "Stimulation Modeling and Circulation Forecasting in the Utah FORGE Doublet" GRC Transactions, 47 (2023).

Nathenson M. "The dependence of permeability on effective stress from fow tests at hot dry rock reservoirs at Rosemanowes (Cornwall) and Fenton Hill (New Mexico)" Geothermics, 28, 315-340, (1999)

Rutquvist, Y.-S., Wu, C.-F, Tsang, G. Bodvarsson, "A modeling approach for analysis of coupled multiphase fluid flow, heat transfer, and deformation in fractured porous rock" International Journal of Rock Mechanics & Mining Sciences, 39, (2002), 429-442.